

# Soft-Phonon Response Function: Inelastic Neutron Scattering from $\text{LaAlO}_3$ <sup>†</sup>

J. K. Kjems and G. Shirane

*Brookhaven National Laboratory, Upton, New York 11973*

K. A. Müller and H. J. Scheel

*IBM Zürich Research Laboratory, 8803 Rüschlikon, Switzerland*

(Received 5 March 1973)

High-resolution inelastic-neutron-scattering measurements have been performed at the cubic-rhombohedral ( $\text{Pm}\bar{3}\text{m} \rightarrow \text{R}\bar{3}\text{c}$ ) phase transitions in a low-mosaic flux-grown single crystal of  $\text{LaAlO}_3$ . The transition occurred at  $(489 \pm 2)^\circ\text{C}$ , somewhat lower than reported for Verneuil-grown samples. The scattering from the soft  $R_{25}$  mode at the corner of the Brillouin zone in the cubic phase exhibits the central component up to  $610^\circ\text{C}$ . In addition, phonon sidebands centered around  $\pm\omega_\infty$  are observed which are overdamped below  $550^\circ\text{C}$ . The observed intensities are well described by a model which relates the central component to the phonon sidebands through an anharmonic coupling parameter  $\delta(T)$ , as recently reported by Shapiro *et al.* for  $\text{SrTiO}_3$ .  $\omega_\infty^2(T)$  is found to deviate from the mean-field behavior near the transition temperature and  $\delta^2(T)$  is found to be nearly constant. A comparison is made between  $\text{LaAlO}_3$ ,  $\text{SrTiO}_3$ , and  $\text{KMnF}_3$  with respect to these parameters as well as the anisotropy of the dispersion surfaces near the  $R$  point.

## I. INTRODUCTION

The structural phase changes in the materials that crystallize in the perovskite structure are often accompanied by soft-phonon modes whose symmetries correspond to the distortion that takes place at the transition.<sup>1</sup> The phase transition in  $\text{LaAlO}_3$  around  $500^\circ\text{C}$  belongs to a class where the condensing mode is found at the  $R$  corner ( $\frac{1}{2}\frac{1}{2}\frac{1}{2}$ ) of the Brillouin zone in the cubic phase.<sup>2</sup> The triply degenerate phonon mode has the  $R_{25}$  irreducible representation<sup>3</sup> and its components can be thought of as alternate librations of the  $\text{AlO}_6$  octahedra around the cubic axis. The low-temperature phase is rhombohedral<sup>4</sup> ( $D_{3d}^6 \equiv \text{R}\bar{3}\text{c}$ ) and the distortion from cubic symmetry corresponds to a condensation of a linear combination of all three cubic components of the  $R_{25}$  mode.<sup>5</sup> Other materials of the same class such as  $\text{SrTiO}_3$  ( $T_c \sim 100\text{ K}$ )<sup>6</sup> and  $\text{KMnF}_3$  ( $T_c \sim 180\text{ K}$ )<sup>7</sup> have a tetragonal distortion in the low-temperature phase resulting from the condensation of only one of the cubic components of the  $R_{25}$  mode. The transitions in  $\text{SrTiO}_3$  and  $\text{LaAlO}_3$  are continuous. Close to the transition the rotation angle of the octahedra, which is the order parameter,<sup>8</sup> shows a deviation from mean-field behavior as measured by EPR.<sup>9</sup>

A neutron-scattering study of  $\text{SrTiO}_3$  by Riste *et al.*<sup>10</sup> has revealed, unexpectedly, a narrow central component in the scattering, in addition to the phonon sidebands. A recent extension of this study including both  $\text{SrTiO}_3$  and  $\text{KMnF}_3$  by Shapiro *et al.*<sup>11</sup> has yielded detailed information on the full response function. It was shown<sup>12</sup> that the soft-phonon frequency  $\omega_\infty$  remains finite at the transition point

and that instead another frequency  $\omega_0$ , which characterizes the total scattering, phonons plus central peak, becomes infinitely small. This behavior is explained in terms of a phenomenological theory which introduces a low-frequency resonance with amplitude  $\delta^2$  in the phonon self-energy and which subsequently relates the characteristic frequencies by  $\omega_0^2 = \omega_\infty^2 - \delta^2$ . The temperature dependence of these parameters could be determined quite close to  $T_c$  in  $\text{SrTiO}_3$  because the phonons remained underdamped, in contrast to  $\text{KMnF}_3$  where the overdamped nature of the phonons prevented detailed quantitative studies. In this respect  $\text{LaAlO}_3$  represents an intermediate case and, since the phase change takes place at a much higher temperature and results in a different low-temperature structure, we expect a quantitative study to yield new information on the central-mode features.

Additional motivation was given by a recent theoretical paper by Enz<sup>13</sup> in which the appearance of the central peak is related to the symmetry of the lowest  $\Gamma$ - $R$  phonon dispersion curve by a touching condition. This curve is nearly symmetric in  $\text{SrTiO}_3$ <sup>6</sup> and in  $\text{KMnF}_3$ <sup>7</sup> but it is asymmetric in  $\text{LaAlO}_3$ ,<sup>2</sup> and, according to the model, a somewhat weaker central peak is expected for the latter case. Our findings of a strong central component very similar to the findings for  $\text{SrTiO}_3$  and for  $\text{KMnF}_3$  most likely do not support this model.

## II. EXPERIMENTAL DETAILS

The measurements were carried out at the Brookhaven high-flux-beam reactor on a triple-axis spectrometer in the constant- $Q$  mode of operation. The spectrometer was equipped with pyro-

lytic graphite monochromator (bent) and analyzer, and filters were used to eliminate the higher-order contamination of the monochromated beam. At 5.1-meV incident energy, the filter was an 8-in. block of polycrystalline beryllium cooled to liquid-nitrogen temperature; at 13.7 meV, pyrolytic graphite single crystals with a total thickness of 4 in. were used; and at 41 meV, 2 in. of pyrolytic graphite served as a filter. The bulk of the measurements were carried out with 20-sec horizontal collimation throughout the spectrometer and the effective vertical resolution was  $1.8^\circ$  [full width at half-maximum (FWHM)]. The resulting high resolution is exemplified by the projection of the resolution ellipsoid on the energy axis (FWHM): 0.08 meV at 5.1-meV incident energy, 0.4 meV at 13.7 meV, and 2.2 meV at 41 meV. The resolution features of a triple-axis spectrometer are well known and they may be reliably simulated on a computer. In the reduction of the data we have used computer programs based on the treatment by Cooper and Nathans<sup>14</sup> and the calculated resolution profiles were checked against measurements at Bragg reflections in the sample.

The  $\text{LaAlO}_3$  single crystal was grown from fluxed melts using lead-based solvents. Several mixtures of  $\text{PbO}$ ,  $\text{PbF}_2$ , and  $\text{B}_2\text{O}_3$  were tried with various ratios of  $\text{La}_2\text{O}_3:\text{Al}_2\text{O}_3$ . The best results were obtained with a  $\text{PbO-PbF}_2$  solvent containing a small amount of  $\text{V}_2\text{O}_5$ . In a typical growth experiment 4.8-g  $\text{La}_2\text{O}_3$  (>99%, Fluka, Buchs/Switzerland), 1.6-g  $\text{Al}_2\text{O}_3$  (high purity, Merck, Darmstadt), 26-g  $\text{PbO}$  and 24-g  $\text{PbF}_2$  (both >99% from Associated Lead Manufacturers, Greenford, Great Britain), and 1-g  $\text{V}_2\text{O}_5$  (>99%, Fluka) were mixed and pre-melted at about  $900^\circ\text{C}$  in a 30-cm<sup>3</sup> platinum crucible. The crucible was sealed with a lid by argon arc welding leaving a hole of less than 0.1 mm for pressure release. Thus evaporation of solvent was minimized. The crucible was placed into a Superkanthal chamber furnace in such a way that a temperature difference of two opposite crucible walls facilitated natural convection, with the coolest spot at the bottom of the crucible. The furnace chamber was then heated to  $1300^\circ\text{C}$  for 15 h, slowly cooled to  $1050^\circ\text{C}$ , heated again to  $1180^\circ\text{C}$  and then cooled at a rate of  $0.5^\circ/\text{h}$  by means of a Eurotherm electronic programmer (ramp generator). The temperature of the heating elements was regulated to  $\pm 0.5^\circ\text{C}$ , and temperature fluctuations in the furnace chamber filled with crucibles and with ceramics were less than  $0.2^\circ\text{C}$ . When the temperature of  $980^\circ\text{C}$  was reached, holes were punched into the lid and excess solution was poured out. The rest of the solidified flux was dissolved in dilute nitric acid.

Three crystals weighing a total of 5.4 g were obtained. The larger two were intergrown at a cor-

ner. The largest crystal of dimensions  $11 \times 9 \times 6$  mm contained few inclusions and cracks and was by more than 95% optically clear. After the corner with the second crystal had been cut off, most of the included flux could be dissolved. This crystal was used in the measurements. The mosaic spread measured in the course of the experiments was less than 6 sec (FWHM). The exceptionally large size of this inclusion-free crystal and the prevention of multinucleation are attributed to the addition of  $\text{V}_2\text{O}_5$  to the solution and could be explained by the formation of  $\text{LaVO}_4$  complexes in the solution and especially in front of the growing crystals where vanadate is rejected. Formation of such complexes extends the width of the metastable Ostwald-Miers region and favors stable growth, and further examples are discussed by Ellwell and Scheel.<sup>15</sup> An electron-microprobe analysis of the crystal showed a locally varying lead concentration between 0.7 and 1.1 wt% and a vanadium content of 0.01–0.02 wt%.

The crystal was mounted with an  $[03\bar{1}]$  axis vertical so that the  $\Gamma$ - $M$  branch was accessible. The transition temperature  $T_c$  was determined from measurements of the scattering at the  $R$  point  $\frac{1}{2}(1,1,3)$  of the cubic Brillouin zone which becomes a reciprocal-lattice point in the distorted phase. The intensity variation on very slow cooling is shown in Fig. 1. The peaking feature at small energy transfers is due to the soft-phonon mode which exists on both sides of  $T_c$  giving rise to a nearly

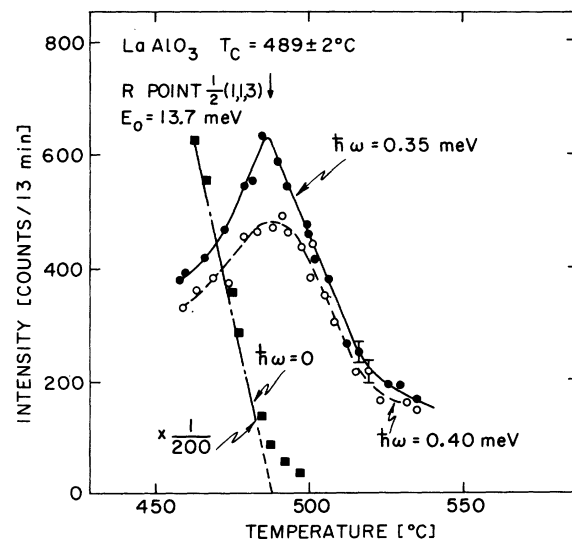


FIG. 1. Determination of the transition temperature at the  $\frac{1}{2}(1,1,3)$   $R$  point. The soft-phonon mode gives rise to a peak in the inelastic scattering at the transition temperature, and the elastic scattering is due to Bragg scattering which only occurs in the distorted phase and to the critical scattering at the phase transition.

symmetric peak as long as elastic Bragg scattering is not picked up by the finite resolution. From these traces a transition temperature of  $(489 \pm 2)^\circ\text{C}$  was deduced. In earlier experiments on Verneuil-grown crystals transition temperatures near  $525^\circ\text{C}$  were reported,<sup>2,4,16</sup> and the difference is probably caused by the lead impurities.

### III. RESPONSE FUNCTION

Microscopic phonon theory with self-consistent treatment of the anharmonic effect is adequate in the description of soft-phonon modes in the temperature ranges where the mean-field approximation is valid. Such a treatment yields the correct temperature dependence of both the order parameter and of the soft-phonon frequency.<sup>13,17,18</sup> However, near the transition temperature where fluctuations are large mean-field theory breaks down and so far only few attempts have been made to calculate the behavior in this regime. Feder<sup>19</sup> has presented thermodynamic arguments for the appearance of a central diffusive mode in the response function and both Silberglitt<sup>20</sup> and Schwabl<sup>21</sup> have shown that microscopic theory assuming a low-frequency resonance in the phonon self-energy also produces a triple-peaked response,<sup>20</sup> but neither approach can actually predict the temperature dependence. This has been done by Schneider, but close to  $T_c$  only.<sup>22</sup> Nevertheless, such theories are useful to the experimentalists in that the derived functional form of the response function can be tried out in fits to experimental observations, and values for the model parameters may be found. In this work we have applied the following form for the response function

$$S(\vec{q}, \omega) = \frac{k_B T}{\pi} \frac{\delta^2(T)}{\omega_0^2(\vec{q}, T) \omega_\infty^2(\vec{q}, T) \omega_0^2 + \gamma'^2} + \frac{k_B T}{\pi} \frac{\Gamma_0}{[\omega_\infty^2(\vec{q}, T) - \omega^2]^2 + \omega^2 \Gamma_0^2}, \quad (1)$$

$$\omega_0^2(\vec{q}, T) \equiv \omega_\infty^2(\vec{q}, T) - \delta^2(T), \quad \gamma' \equiv \gamma(\omega_0/\omega_\infty)^2,$$

which is derived under the conditions that  $\Gamma_0 \ll \delta^2/\gamma$  and  $\omega_\infty^2 \gg \gamma^2$  and which obeys the following sum rule:

$$\int_{-\infty}^{\infty} S(\vec{q}, \omega) d\omega = \frac{1}{\omega_0^2(\vec{q}, T)} = \frac{\delta^2(T)}{\omega_0^2(\vec{q}, T) \omega_\infty^2(\vec{q}, T)} + \frac{1}{\omega_\infty^2(\vec{q}, T)}. \quad (2)$$

The first term in Eq. (1) represents the central peak and the second term represents the phonon bands at  $\pm \omega_\infty(\vec{q}, T)$ . This form results from the incorporation of the simplest possible low-frequency resonance at frequency  $\gamma$  in the self-energy with the amplitude  $\delta^2(T)$ . The arithmetic derivation of Eq. (1) is given by Shapiro *et al.*<sup>11</sup> It relates with a single parameter  $\delta^2(T)$  both the amplitude and the  $\vec{q}$  dependence of the central peak to the phonon bands, and it was shown to give an adequate description of the observed intensities near the phase transition in the cubic phase of  $\text{SrTiO}_3$ . Shapiro *et al.* pointed out the paramount importance of the resolution effects when dealing with very singular cross sections such as Eq. (1) and in the following we wish to extend their discussion.

Given a functional form of the cross section the expected intensities may be calculated by a folding with four-dimensional resolution function  $R(\vec{q}, \omega)$ :

$$I_j(\vec{q}_0, \omega) = A(k_i/k_f) |F_j(\vec{\kappa})|^2 \int d\vec{q} d\omega S(\vec{q}, \omega) \times R(\vec{q} - \vec{q}_0, \omega - \omega_0), \quad (3)$$

where  $\vec{\kappa}_i$  and  $\vec{\kappa}_f$  are the initial and final wave vectors of the scattered neutrons  $\vec{\kappa} = \vec{\kappa}_i - \vec{\kappa}_f$ , and  $F_j(\kappa)$  is the inelastic structure factor for the  $j$ th mode at  $\vec{q} = \vec{\kappa} - \vec{\tau}$ ,  $\vec{\tau}$  being a reciprocal-lattice vector. Equation (3) shows that the observed intensities even in constant- $q$ -scans with  $\vec{q}_0 = 0$  will depend on the behavior of  $S(\vec{q}, \omega)$  at finite  $\vec{q}$  which means that we have to insert some information about the dispersion around the  $R$  point in our fitting attempts to the soft-mode response function. Gesi *et al.*<sup>7</sup> have shown that the dispersion of the triply degenerate  $R_{25}$  mode to a good approximation is given by the following truncated dynamical matrix which neglects all other degrees of freedom than the librations of the  $\text{AlO}_6$  octahedra:

$$\vec{D}(\vec{q}_R + q) = \begin{pmatrix} \omega_\infty^2 + \lambda_1 q_x^2 + \lambda_2 (q_y^2 + q_z^2) & \lambda_3 q_x q_y & \lambda_3 q_x q_z \\ \lambda_3 q_x q_y & \omega_\infty^2 + \lambda_1 q_y^2 + \lambda_2 (q_x^2 + q_z^2) & \lambda_3 q_y q_z \\ \lambda_3 q_x q_z & \lambda_3 q_y q_z & \omega_\infty^2 + \lambda_1 q_z^2 + \lambda_2 (q_x^2 + q_y^2) \end{pmatrix}. \quad (4)$$

A comparison of the above form of the dynamical matrix to a small- $q$  expansion of the form derived by Pytte and Feder<sup>17</sup> by self-consistent anharmonic theory shows that the correlation functions which determine the temperature dependence of  $\omega_\infty^2$  also enter in the expressions for  $\lambda_i$ . However, meaningful estimates of the temperature variation of  $\lambda_1$

cannot be obtained from this theory because the results depend crucially on the assumed force constants. Detailed knowledge of the dispersion near the  $R$  point at temperatures close to  $T_c$  in  $\text{LaAlO}_3$  is not experimentally accessible owing to the overdamped nature of the phonons, and so the information we are able to extract about the soft-mode re-

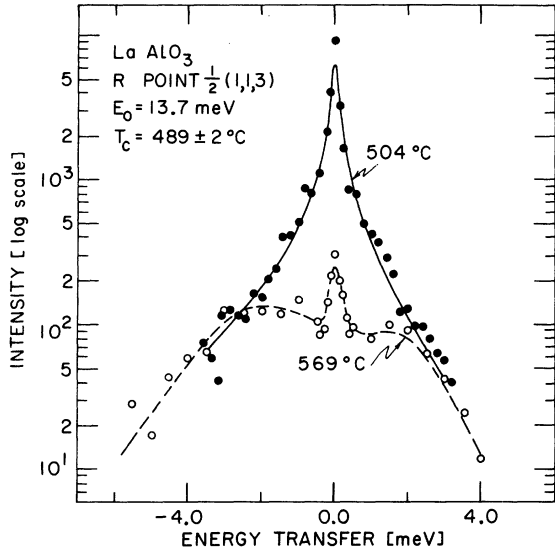


FIG. 2. Observed intensities at 13.7-meV incident neutron energy. The broken and full lines represent the best fit to the data using Eq. (1) of the text with the appropriate resolution corrections.

sponse function will be limited by this deficiency. To illustrate how the uncertainty in the values of  $\lambda_i$  introduces uncertainties in the derived model parameters, we may perform an integration of the central-peak cross section [Eq. (2)] along the vertical component of  $\vec{q}$ ; the integration is inherent to the experiment due to the relaxed vertical collimation. We also integrate over  $\omega$  since the width of the central peak is always found much smaller than the instrumental energy resolution. The result is

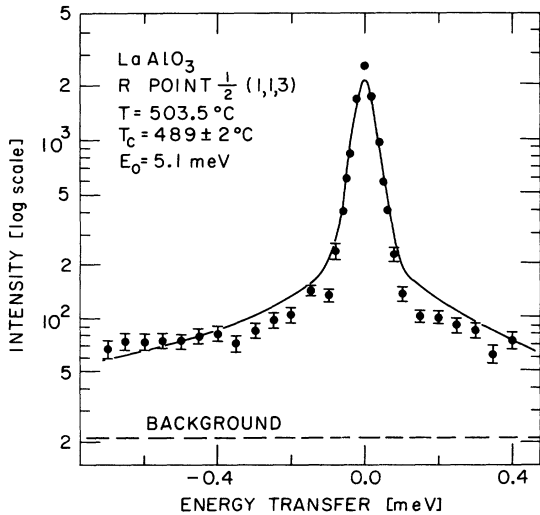


FIG. 3. Observed intensities at 5.1-meV incident neutron energy. The full line is calculated on the basis of the parameters derived from fits to the 13.7-meV data.

$$S_{\text{centr.}}(\vec{q}_s) = \int d\omega dq_x S_{\text{centr.}}(\vec{q}, \omega) = \frac{\delta^2(T)}{[\lambda_2(T)]^{1/2}} \times \frac{k_B T}{\omega_\infty^2(\vec{q}_s, T)\omega_0(\vec{q}_s, T) + \omega_\infty(\vec{q}_s, T)\omega_0^2(\vec{q}_s, T)}, \quad (5)$$

where  $\vec{q}_s$  lies in the scattering plane. It shows that  $\delta^2(T)$  can only be determined to the accuracy of our knowledge of  $[\lambda_2(T)]^{1/2}$ .

#### IV. RESULTS AND DISCUSSION

The existence of a central component in the response function of the soft  $R_{25}$  mode in cubic  $\text{LaAlO}_3$  is convincingly seen in Figs. 2 and 3, which also illustrates the influence of the finite resolution on the observed line shapes. At 13.7-meV incident energy, only in the high-temperature scan in Fig. 2 are the phonon bands and the central peak distinct; however, at 5.1-meV incident energy, we still can distinguish the narrow central component from the phonons at the lower temperature as seen in Fig. 3. It is noted that a small amount of incoherent scattering has been subtracted from the data so that the central feature is entirely due to the response function. The rapid temperature variation of the central peak is illustrated in Fig. 4 where the inverse peak intensity (extrapolated

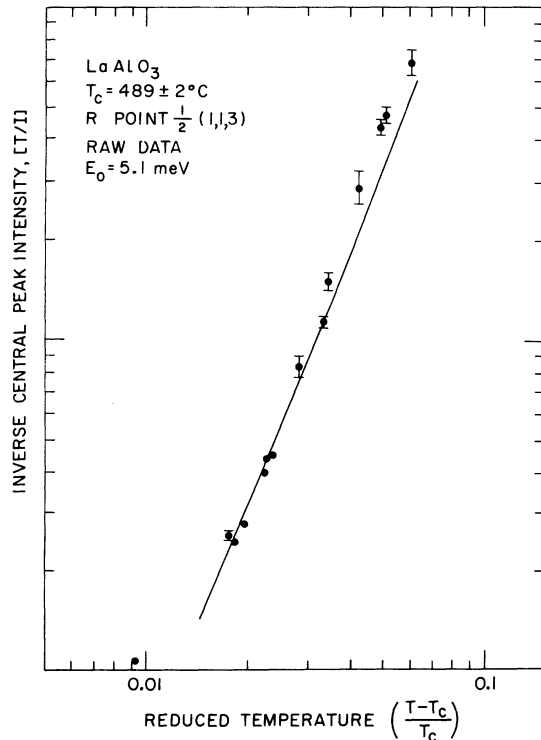


FIG. 4. Temperature over the observed peak intensity of the central component plotted on double logarithmic scale vs the reduced temperature. The solid line is based on the lines drawn through the data points in Fig. 6.

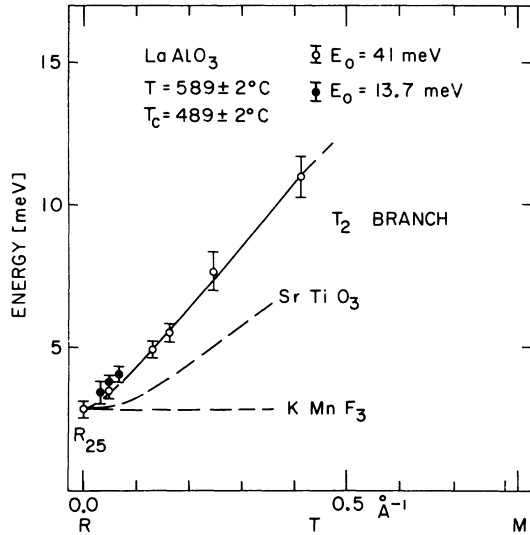


FIG. 5. Dispersion of the lowest phonon branch along  $R$  to  $M$  on the edge of the Brillouin zone. The dispersion of the equivalent branches in  $\text{KMnF}_3$  and  $\text{SrTiO}_3$  is indicated for comparison.

phonon background subtracted) is plotted against the reduced temperature. For  $(T - T_c)/T_c > 0.02$  the  $q_s$  width of the central peak is larger than the  $q_s$  width at zero-energy transfer of the resolution function, whereas the energy width is smaller than the resolution width so as an approximation we may use Eq. (5) to describe the peak intensity variation. This is done for the solid line using the parameters derived below.

In order to obtain the dispersion parameters for the fitting procedure we measured the dispersion of the lowest  $R$ - $M$  branch in the cubic phase  $100^\circ\text{C}$  above the transition and the result is shown in Fig. 5. Together with previous measurements by Axe *et al.*<sup>2</sup> along the  $\Gamma$ - $R$  direction our data yielded the following parameters  $\lambda_1 = \lambda_2 = 2000 \text{ meV}^2 \text{ \AA}^2$ . These isotropic values were used at all temperatures together with the assumption  $\lambda_3 = 0$ . Also, in Fig. 5 we have as a comparison indicated the dispersion of the equivalent branch in  $\text{KMnF}_3$  and  $\text{SrTiO}_3$ . Our finding of a nearly isotropic dispersion in  $\text{LaAlO}_3$  as opposed to the marked anisotropy found most pronounced in  $\text{KMnF}_3$  but also in  $\text{SrTiO}_3$  may intuitively be related to the fact that the latter two undergo a tetragonal distortion at the phase change whereas  $\text{LaAlO}_3$  distort rhombohedrally. However, mean-field theory does not show such a connection.

The soft phonon was followed at  $\frac{1}{2}(1, 1, 3)$  in the temperature range  $500$ – $600^\circ\text{C}$  and, independent of the central peak, the damped harmonic oscillator response was fitted to the observed phonon intensities using  $\Gamma_0$  and  $\omega_\infty^2$  as variables. Below  $550^\circ\text{C}$ ,

the response is overdamped and no shoulders were explicit in the data. The fits were still reliable down to  $530^\circ\text{C}$  since the scaling factor was already determined at high temperatures and the separation of the central peak was readily made. The broken line in Fig. 2 gives an example of the fitted curves. After the phonon parameters were determined only  $\delta^2(T)$  was allowed to vary in order to fit the central peak. Below  $530^\circ\text{C}$  the full cross section was used and the full line in Fig. 2 represent the best fit to the  $504^\circ\text{C}$  data. The same parameters except for a scaling parameter were used to draw the full line through the higher resolution data on Fig. 3 and the consistency is satisfactory but not overwhelming, the main reason being the approximate way in which the dispersion is taken into account in the resolution correction. It is seen that the central component is calculated too broad which indicates that the value used for  $\lambda_i$  is too small but the data do not contain enough information to include  $\lambda_i$  as parameters to be fitted. At  $569^\circ\text{C}$  where the  $q$  width of the central peak is much larger than the instrumental resolution, we measured the  $q$  profile and the observed full width of  $0.068 \pm 0.008 \text{ \AA}^{-1}$  compared well with the calculated value of  $0.072 \text{ \AA}^{-1}$  based on the derived cross-section parameters. The results of the fits for  $\omega_\infty^2$  and  $\delta^2$  are shown in Fig. 6. The error bars only refer to the statistical uncertainty in the determination. The phonon width was found to be essentially constant through the temperature range  $\Gamma_0 = 2.8 \pm 0.2 \text{ meV}$  and the fits were quite insensitive to the value of  $\gamma'$  as long as it was smaller than half the resolution width so values of  $0.02$  and  $0.03$

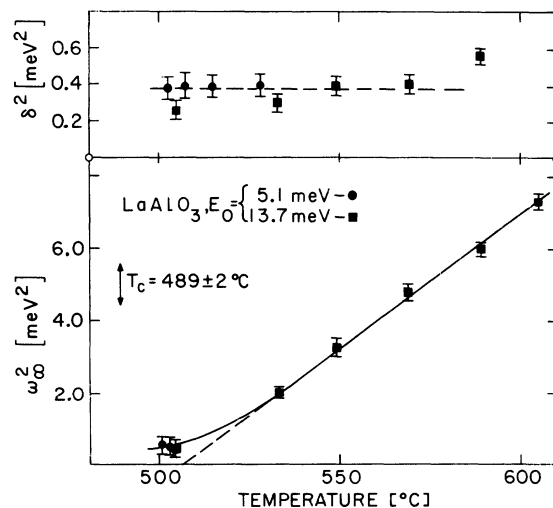


FIG. 6. Temperature dependence of the parameters  $\omega_\infty^2$  and  $\delta^2$  of the response function as determined by the least-squares-fitting procedure. The error bars do not include systematic error.

meV were used but these values can only be taken as crude upper limits for the actual  $\gamma'$ . Recent analysis of the EPR line width of the  $\text{Fe}^{3+}-V_0$  center in  $\text{SrTiO}_3$  has shown that  $\gamma'$  ( $\rho$  in Ref. 23) 0.8 °C above  $T_c$  is above 70 MHz which is more than one order of magnitude below the resolution of the present neutron spectrometers.

The general picture that emerges of the response function associated with the soft mode in  $\text{LaAlO}_3$  is similar to the findings for  $\text{SrTiO}_3$  and  $\text{KMnF}_3$  in spite of the fact that the transition temperature is much higher. Away from  $T_c$ ,  $\delta^2$  is constant and  $\omega_{\infty}^2$  varies linearly with temperature but extrapolates to zero well above the observed transition temperature. Near  $T_c$  a relatively rapid temperature variation of  $\delta^2$  (from 0.9 to 0.4  $\text{meV}^2$ ) is found in  $\text{SrTiO}_3$  of which we find no indication in  $\text{LaAlO}_3$ ;

however, we could not derive meaningful parameters in the immediate vicinity of  $T_c$  where the phonon is extremely overdamped. Within the limitations set by the uncertainty in the dispersion parameters we find that the phenomenological form of the response function as given by Eq. (1) is an adequate representation of the observed scattering. Further theoretical work is needed to elucidate the temperature dependence of the involved parameters.

#### ACKNOWLEDGMENTS

Stimulating discussions with J. D. Axe, S. M. Shapiro, and E. Steigmeier are gratefully acknowledged. The authors would like to thank J. Sommerauer, ETH, Zürich, for the microprobe analysis, and W. Berlinger for cutting the crystal.

<sup>†</sup>Work performed under the auspices of the U. S. Atomic Energy Commission.

<sup>1</sup>For listing of soft-mode materials see, for example, G. Shirane, in *Structural Phase Transitions and Soft Modes*, edited by E. J. Samuelsen, E. Andersen, and J. Feder (Universitetsforlaget, Oslo, Norway, 1971), pp. 217-234.

<sup>2</sup>J. D. Axe, G. Shirane, and K. A. Müller, *Phys. Rev.* **183**, 820 (1969).

<sup>3</sup>The original nomenclature introduced by R. A. Cowley [*Phys. Rev.* **134**, A981 (1964)] was  $\Gamma_{25}$  because the  $R$  point has the same point symmetry as the origin. However, it seems appropriate to emphasize that it is a zone-boundary mode by using the notation  $R_{25}$ .

<sup>4</sup>K. A. Müller, W. Berlinger, and F. Waldner, *Phys. Rev. Lett.* **21**, 814 (1968).

<sup>5</sup>W. Cochran and A. Zia, *Phys. Status Solidi* **25**, 273 (1968).

<sup>6</sup>G. Shirane and Y. Yamada, *Phys. Rev.* **177**, 858 (1969).

<sup>7</sup>K. Gesi, J. D. Axe, G. Shirane, and A. Linz, *Phys. Rev. B* **5**, 1933 (1972).

<sup>8</sup>W. Cochran, in Ref. 1, pp. 1-14.

<sup>9</sup>K. A. Müller and W. Berlinger, *Phys. Rev. Lett.* **26**, 13 (1971).

<sup>10</sup>T. Riste, E. J. Samuelsen, K. Otnes, and J. Feder, *Solid State Commun.* **9**, 1455 (1971).

<sup>11</sup>S. M. Shapiro, J. D. Axe, G. Shirane, and T. Riste, *Phys. Rev. B* **6**, 4332 (1972).

<sup>12</sup>G. Shirane and J. D. Axe, *Phys. Rev. Lett.* **27**, 1803 (1971).

<sup>13</sup>C. P. Enz, *Phys. Rev. B* **6**, 4695 (1972).

<sup>14</sup>M. J. Cooper and R. Nathans, *Acta Cryst.* **23**, 357 (1967).

<sup>15</sup>D. Elwell and H. J. Scheel, *Crystal Growth from High Temperature Solutions* (Academic, London, to be published).

<sup>16</sup>V. Plakhty and W. Cochran, *Phys. Status Solidi* **29**, 1281 (1968).

<sup>17</sup>E. Pytte and J. Feder, *Phys. Rev.* **187**, 1077 (1969); *Phys. Rev. B* **1**, 4803 (1970).

<sup>18</sup>B. Pietrass, *Phys. Status Solidi* **53**, 279 (1972).

<sup>19</sup>J. Feder, *Solid State Commun.* **9**, 2021 (1971).

<sup>20</sup>R. Silbergliitt, *Solid State Commun.* **11**, 247 (1972).

<sup>21</sup>F. Schwabl, *Z. Phys.* **254**, 57 (1972).

<sup>22</sup>T. Schneider, *Phys. Rev. B* **7**, 201 (1972).

<sup>23</sup>Th. v. Waldkirch, K. A. Müller, and W. Berlinger, *Phys. Rev. B* (to be published).